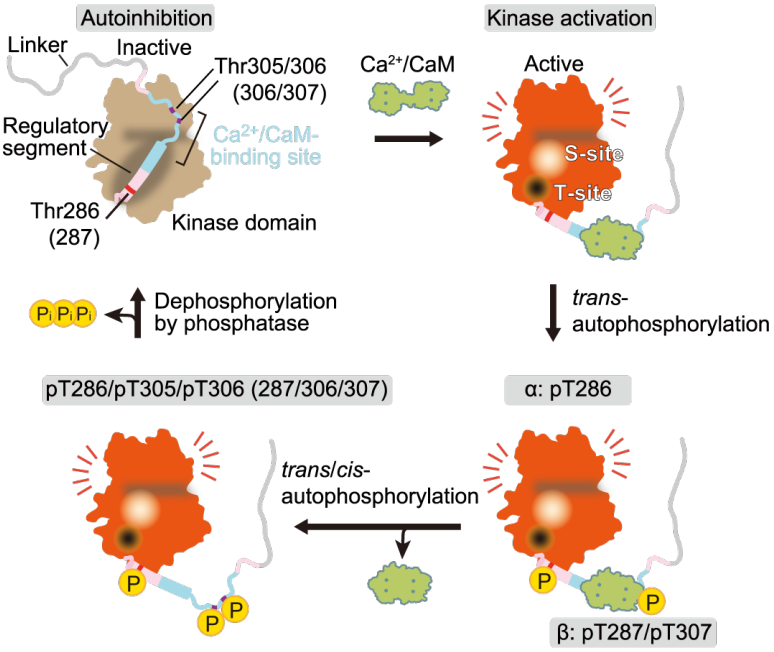

Supplementary Fig. 1: Activation state of a kinase domain in CaMKII

Illustration of the state change of CaMKII, focusing on a single kinase domain. In the inactive state, the kinase domain is autoinhibited by the regulatory segment (autoinhibition). The binding of Ca^{2+}/CaM leads to the release of this regulatory segment, revealing the substrate-binding site (S-site; orange) and the GluN2B-binding site (T-site; black) (i.e., kinase activation). The concomitant activation of adjacent kinases results in autophosphorylation at Thr286 (pT286). Our experiments showed that both The287 and Thr307 are phosphorylated in CaMKIIβ (pT287/pT307). Following the dissociation of Ca^{2+}/CaM, autophosphorylation occurs at Thr305/306 (Thr306/307). Ultimately, a protein phosphatase dephosphorylates CaMKII, returning it to the inactive state. The numbers in parentheses refer to CaMKIIβ.

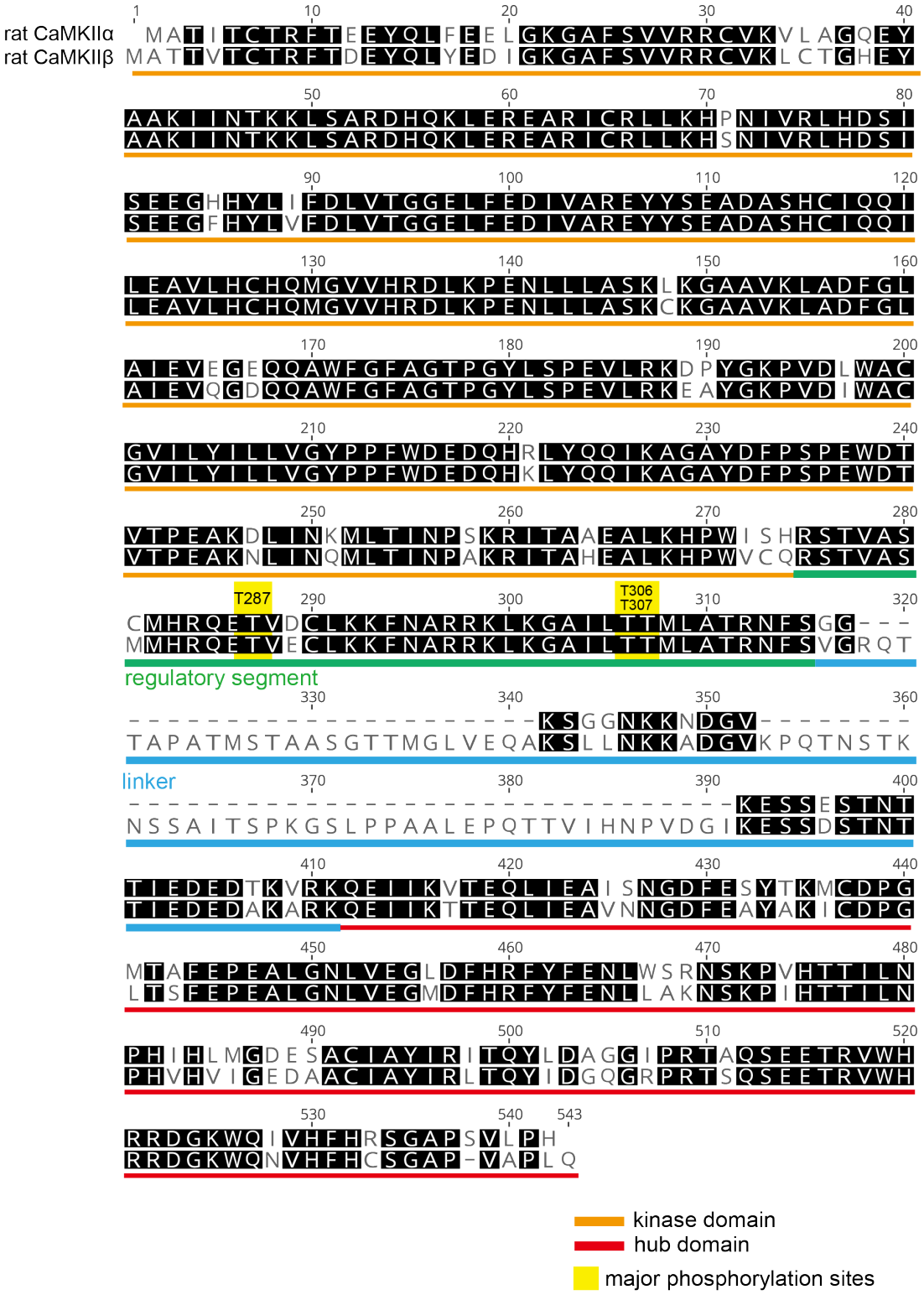

Supplementary Fig. 2: Sequence alignment of the rat CaMKIIα and CaMKIIβ used in this study.

rat CaMKIIα (*Rattus norvegicus*, Accession#: NP_037052.1) and rat CaMKIIβ (*Rattus norvegicus*, Accession#: NP_ 068507.2).

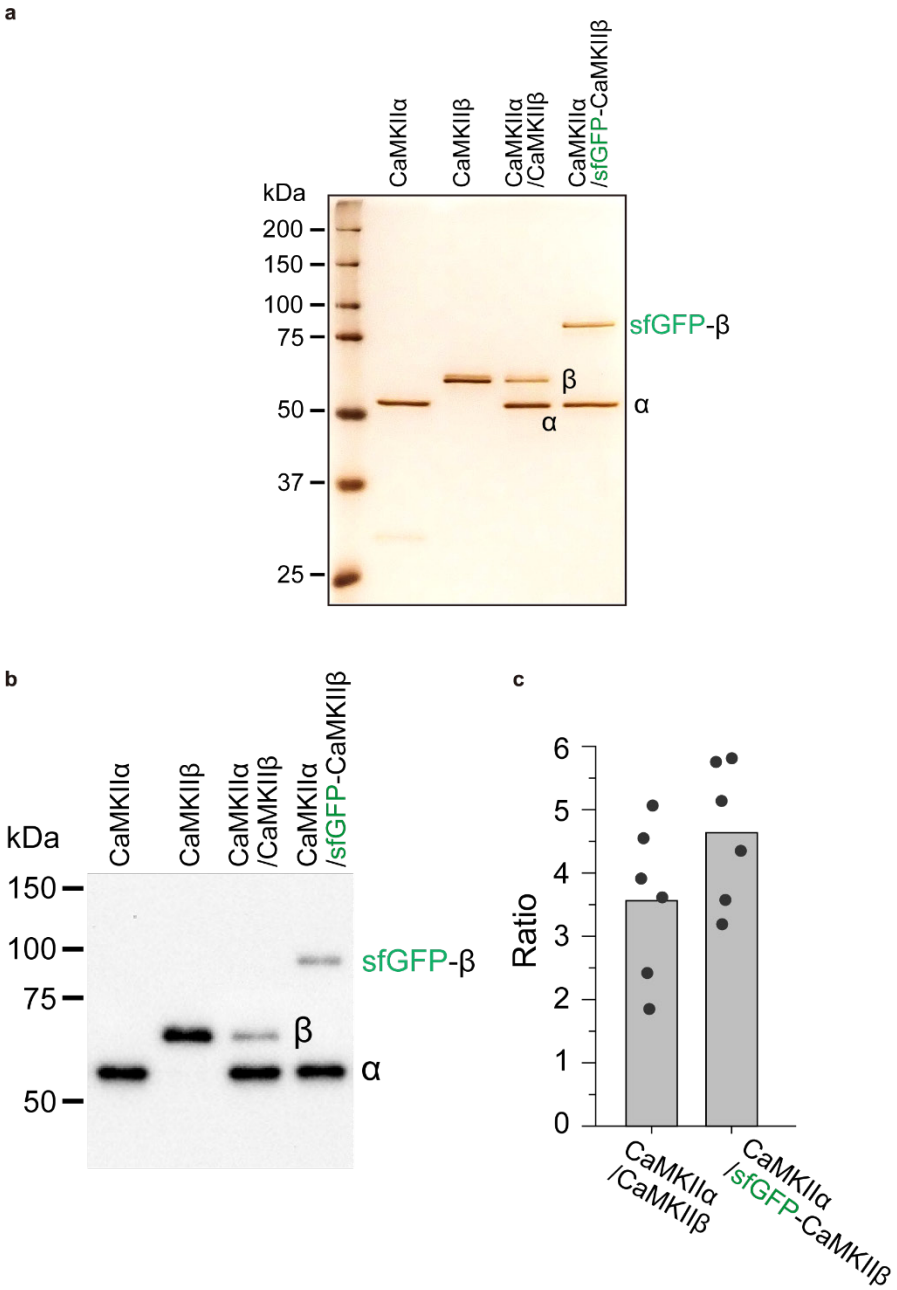

Supplementary Fig. 3: Biochemical validation of purified CaMKII proteins

a, The purity of CaMKII proteins was confirmed by silver staining. CaMKII holoenzymes in the absence of ADP/ATP were purified from HEK-293 cells via two-step purification with His and Strep tags.

b,**c**, The ratio of CaMKIIα to CaMKIIβ in the purified proteins containing both isoforms was determined by western blotting (**b**), and the band intensities were quantified ($n = 6$, technical replicates) (**c**). Source data are provided as a Source Data file.

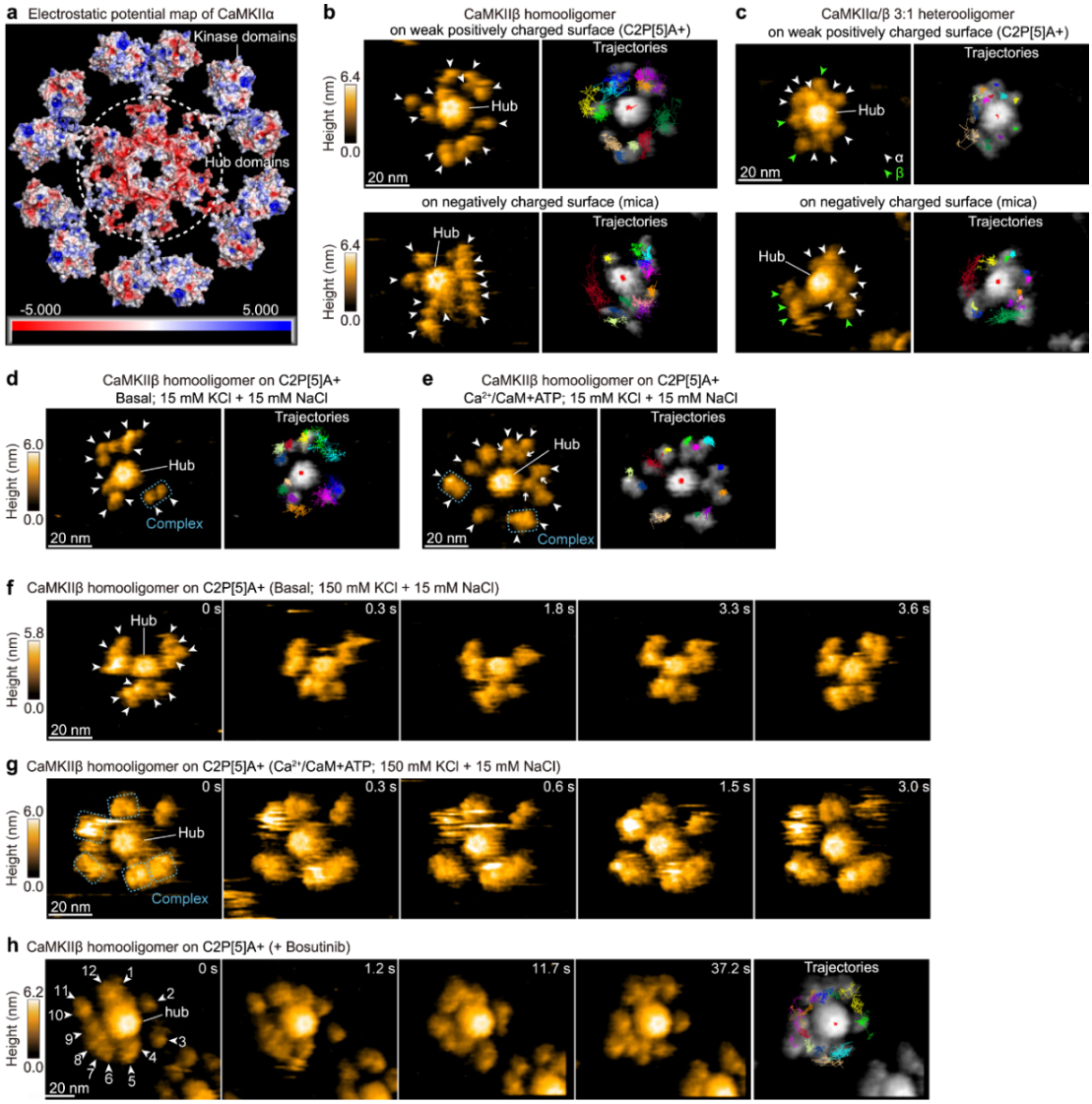

Supplementary Fig. 4: Optimization of HS-AFM observations of CaMKII oligomers

a, Electrostatic potential map of CaMKIIα, which is based on a pseudoatomic model derived from EM data[21].

b–e, HS-AFM images of CaMKIIβ homooligomers and CaMKIIα/β heterooligomers adsorbed on mica surfaces (**b**, **c**) and under different buffer conditions (**d**, **e**). Frame rate, 3.3 frames/s. The trajectories of the kinase domains and the center of the hub assembly (red in the center) were tracked for approximately 40 s (also in **h**).

f–g, Sequential HS-AFM images of CaMKIIβ homooligomers in the basal state (**f**) and under Ca^{2+}/CaM + ATP conditions (**g**) with high salt concentrations in 15 mM NaCl buffer.

h, Sequential HS-AFM images of CaMKIIβ in the presence of 50 μM bosutinib (see also Supplementary Movie 2). The white arrowheads indicate kinase domains, each arbitrarily numbered. Frame rate, 3.3 frames/s. The trajectories of the kinase domains and the center of the hub assembly (red in the center) were tracked for approximately 40 s. HS-AFM experiments were independently repeated at least three times with similar results.

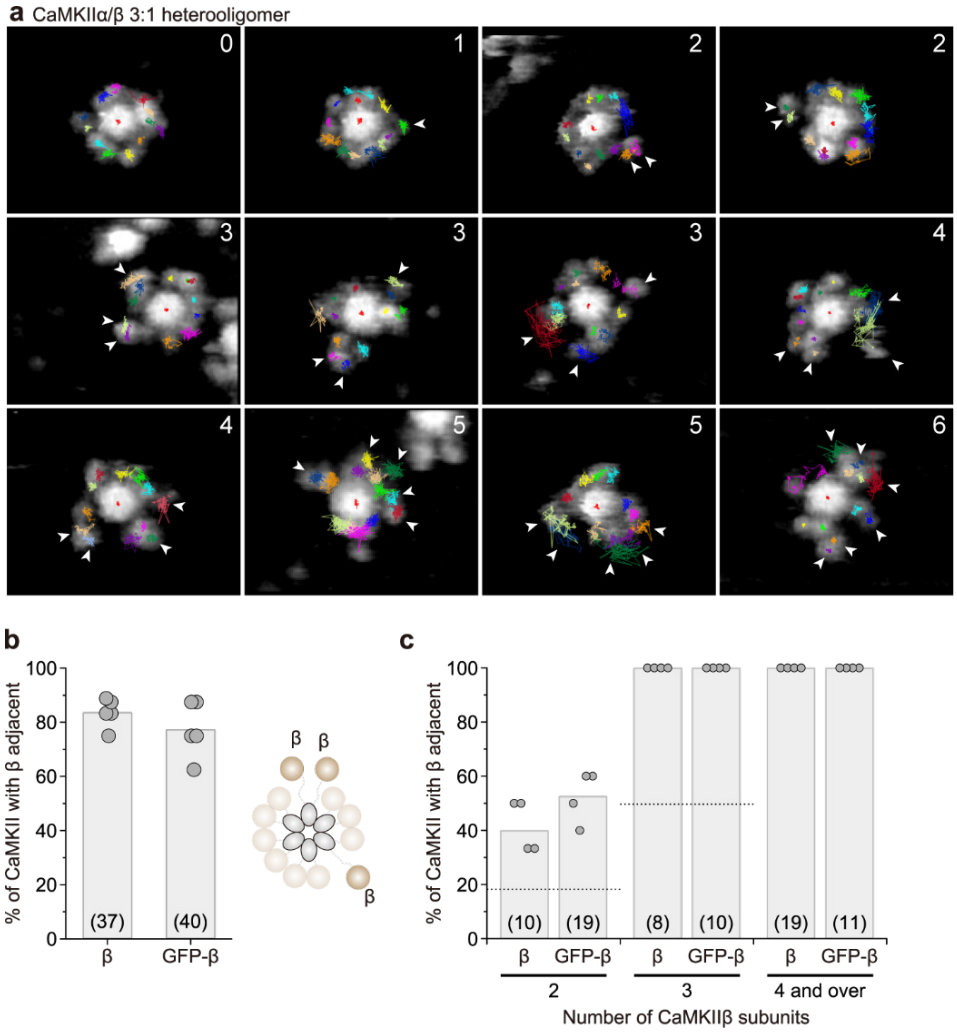

Supplementary Fig. 5: The CaMKIIα/β heterooligomer consists of a 12-meric ring containing both CaMKIIα and CaMKIIβ subunits, with the CaMKIIβ subunits positioned adjacent to one another

a, Trajectories of the kinase domains and the center of the hub assembly (red in the center) of the CaMKIIα/β heterooligomer (approximately 30 s). Frame rate, 3.3 frames/s. The white arrowheads indicate kinase domains derived from CaMKIIβ subunits. The numbers in the upper right indicate the number of CaMKIIβ subunits (see the Methods for the criteria used to determine the number of CaMKIIβ subunits). HS-AFM experiments were independently repeated at least three times with similar results.

b, Percentages of neighboring CaMKIIβ and GFP-CaMKIIβ subunits within a CaMKIIα/β 12-meric ring ($n = 5$, technical replicates). The numbers in parentheses indicate the number of analyzed oligomers (also in **c**). Bar charts show the average (also in **c**).

c, Percentages of neighboring CaMKIIβ subunits and GFP-CaMKIIβ subunits within a CaMKIIα/β 12-meric ring according to the number of CaMKIIβ subunits ($n = 4$, technical replicates). For two or three subunits, probabilities calculated as random chance are shown as dotted lines. Source data are provided as a Source Data file.

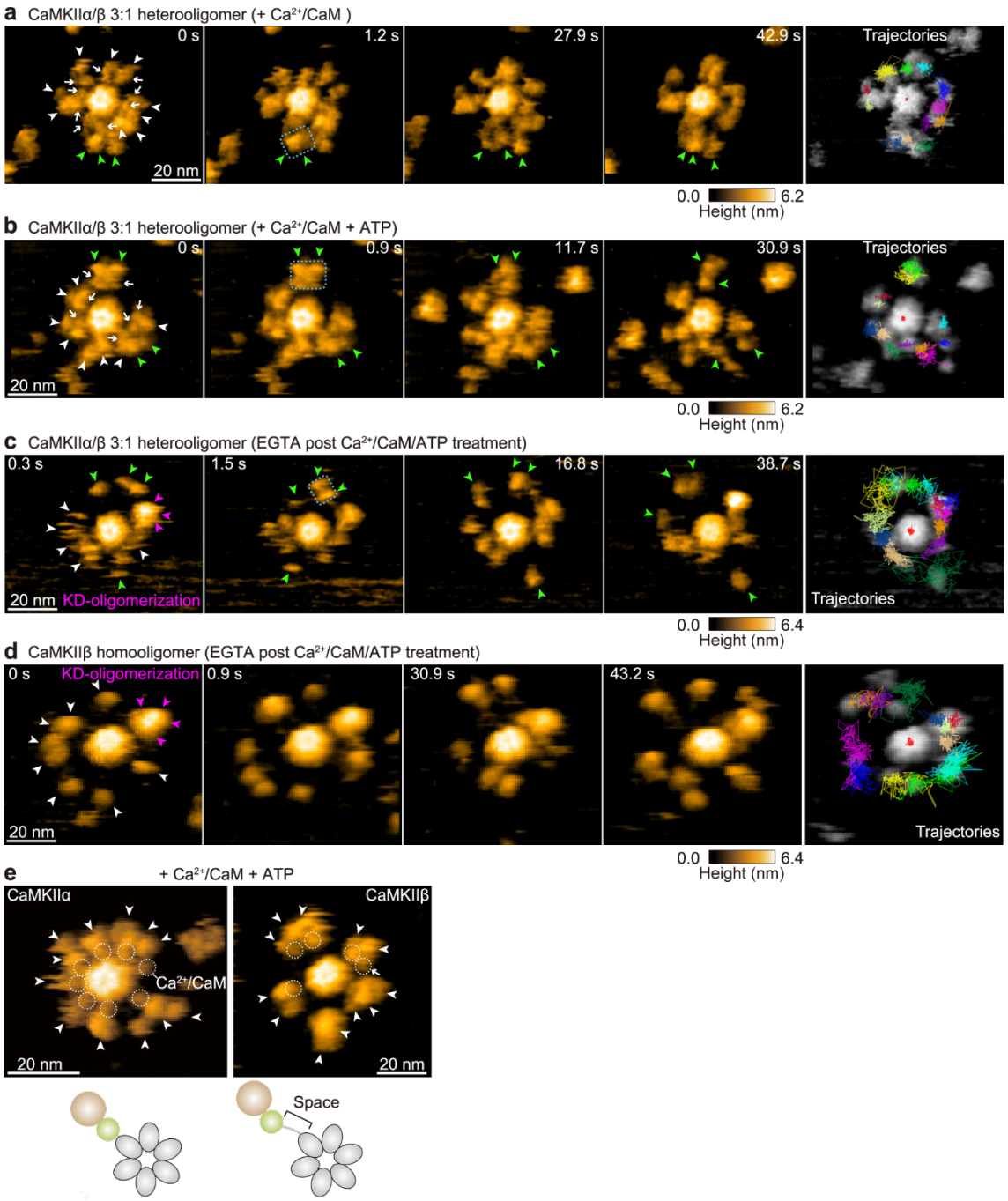

Supplementary Fig. 6: HS-AFM observations of the activation states of the CaMKIIα/β heterooligomer

a-d, Sequential HS-AFM images of Ca^{2+}/CaM-bound CaMKIIα/β heterooligomers (**a**; 1 mM Ca^{2+}, 800 nM CaM; see also Supplementary Movie 6), pT286(287) CaMKIIα/β heterooligomers (**b**; 1 mM Ca^{2+}, 800 nM CaM, and 1 mM ATP; see also Supplementary Movie 8), pT286(287)/pT305(306)/pT306(307) CaMKIIα/β heterooligomers (**c**; see also Supplementary Movie 10), and pT287/pT306/pT307 CaMKIIβ (**d**; see also Supplementary Movie 9). The white arrows indicate Ca^{2+}/CaM bound to the kinase domains (see the

Materials for the criteria used to determine the CaMKIIβ subunits). The white and green arrowheads indicate kinase domains derived from the CaMKIIα and CaMKIIβ subunits, respectively. The blue dotted squares indicate a kinase domain complex. Magenta arrowheads indicate KD-oligomerization. Frame rate, 3.3 frames/s. The trajectories of the kinase domains and the center of the hub assembly (red in the center) were tracked for approximately 45 s.

e, Comparison of HS-AFM images of CaMKIIα and CaMKIIβ homooligomers in the presence of Ca^{2+}/CaM and ATP. White dotted circles indicate Ca^{2+}/CaM. The bottom figure shows the distance between the Ca^{2+}/CaM-bound kinase domain and the hub domain, revealing that a space exists in CaMKIIβ. HS-AFM experiments were independently repeated at least three times with similar results.

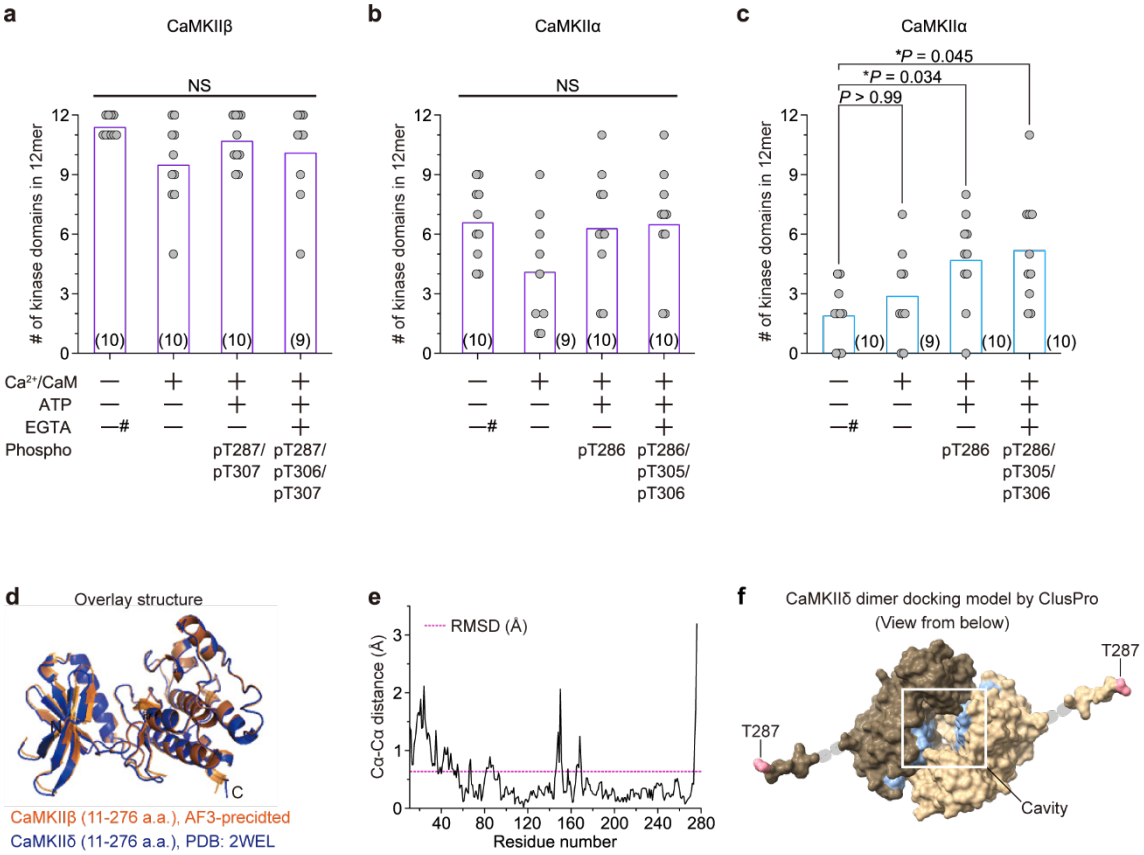

Supplementary Fig. 7: The kinase domains of CaMKIIβ assemble into multiple stable complexes in the 12-meric ring

a,**b**, The number of kinase domains that formed complex states in the 12-meric ring per CaMKIIβ (**a**) and CaMKIIα (**b**) homooligomer under the indicated conditions. The number in parentheses is the number of holoenzymes used in the analysis (Kruskal–Wallis test). Bar charts show the average (also in **c**). #: 0.1 mM EGTA (also in **c**).

c, The number of kinase domains that remained in the complex state for more than 45 s per 12-meric CaMKIIα homooligomer under the indicated conditions. The number in parentheses is the number of holoenzymes used in the analysis (Kruskal–Wallis test with Dunn's post hoc test).

d, Overlaid structure of AF3-predicted CaMKIIβ (residues 11–276) and CaMKIIδ/Ca^{2+}/CaM kinase domains.

e, Cα-Cα distance and root-mean-square deviation (RMSD) of Cα positions between the kinase domains of AF3-predicted CaMKIIβ and CaMKIIδ/Ca^{2+}/CaM.

f, Dimer model derived from protein–protein docking of the CaMKIIδ/Ca^{2+}/CaM kinase domain. All tests are two-tailed (**a**-**c**). NS, not significant ($P > 0.05$); $^{*}P < 0.05$ (**a**-**c**). Source data are provided as a Source Data file.

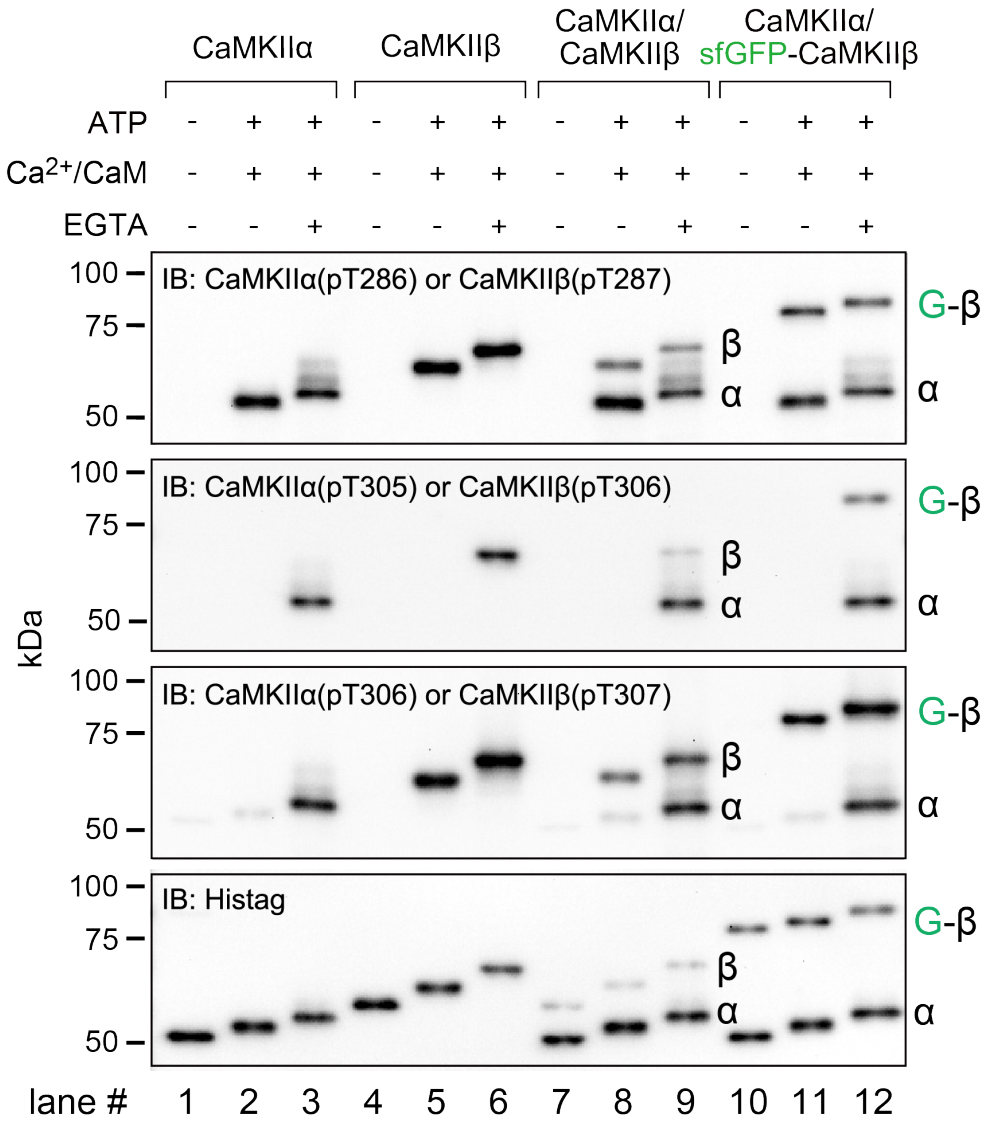

Supplementary Fig. 8: Phosphorylation of purified CaMKII

(lanes #1, 4, 7, 10) Purified proteins were loaded without activation.

(lanes #2, 5, 8, 11) CaMKII proteins (50 nM) were incubated with 800 nM CaM, 1 mM $CaCl_2$, and 1 mM ATP in reaction buffer (50 mM Tris-HCl, pH 7.4; 50 mM KCl; and 10 mM $MgCl_2$) at 30°C for 5 min. This protocol selectively induces phosphorylation at Thr286 of CaMKIIα and Thr287/Thr307 of CaMKIIβ.

(lanes #3, 6, 9, 12) Ca^{2+}/CaM was dissociated by incubation with 2 mM EGTA for 5 min at 30°C and an additional 10 min at 25°C. This protocol induces the phosphorylation of CaMKIIα at Thr286/305/306 and CaMKIIβ at Thr287/306/307. The amount of protein loaded was assessed with an anti-His tag antibody. Source data are provided as a Source Data file.

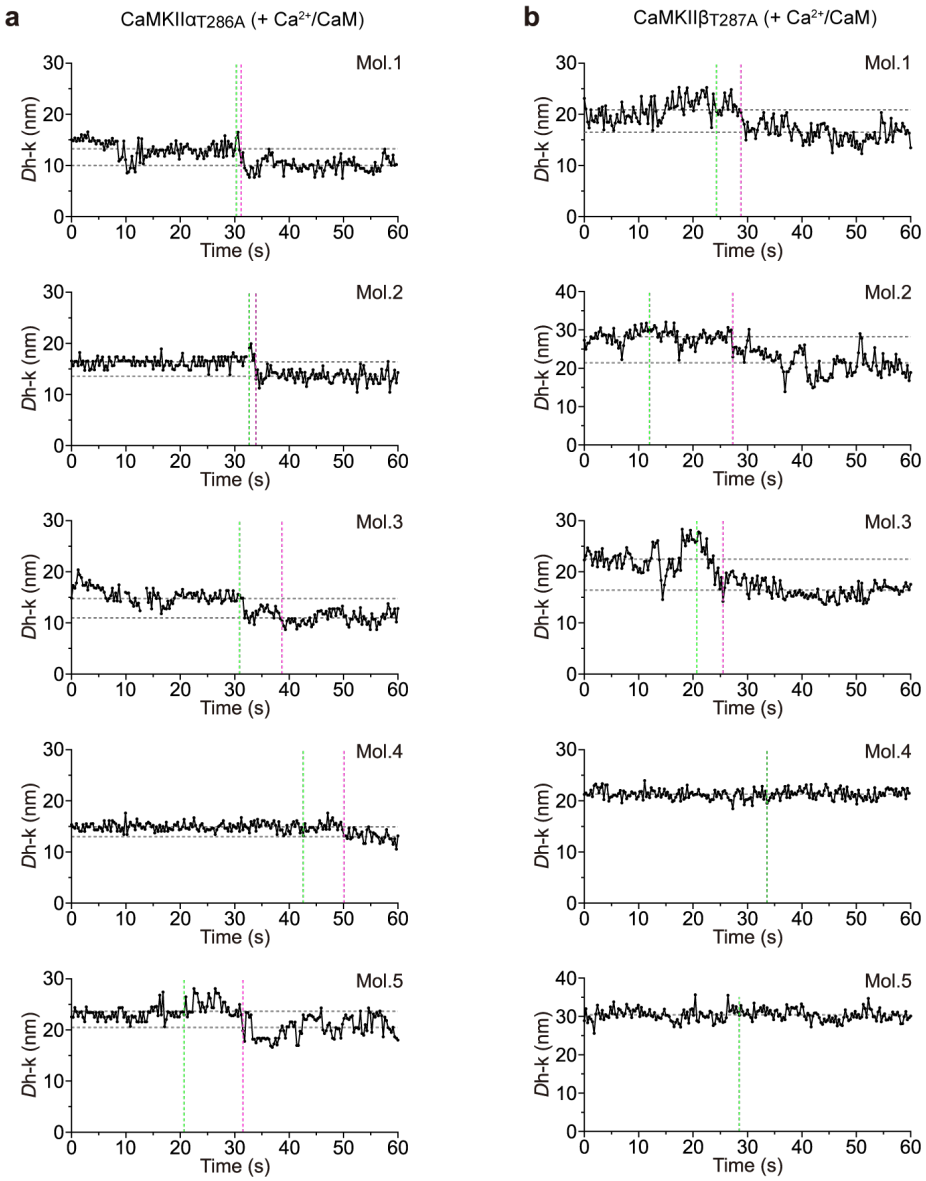

Supplementary Fig. 9: Kinase domain complexes formed in the activated state exhibit slow structural decay to the basal state after Ca^{2+}/CaM dissociation

a,**b**, Five representative distances from the center of the hub assembly to kinase domains ($D_{h\text{-}k}$) as a function of time for CaMKIIα$_{T286A}$ (**a**) and CaMKIIβ$_{T287A}$ (**b**). The magenta and green dotted lines indicate the events of Ca^{2+}/CaM dissociation and kinase domain contraction, respectively. The gray dotted lines indicate the average $D_{h\text{-}k}$ before and after kinase domain contraction. Source data are provided as a Source Data file.

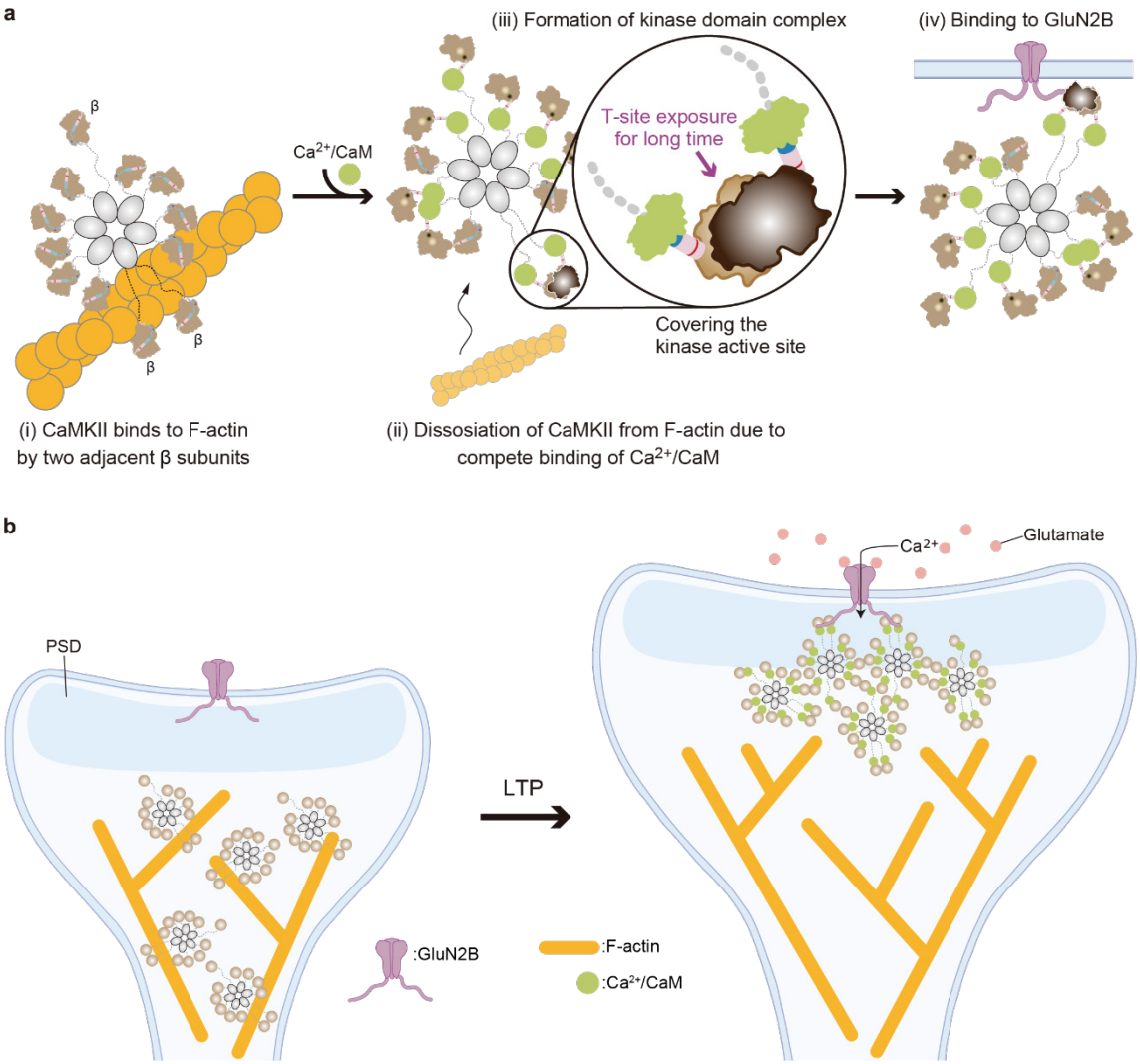

Supplementary Fig. 10: Model of the activation of CaMKIIα/β heterooligomers in the spine

a, Depicted the transition of binding of CaMKIIα/β heterooligomers from F-actin to GluN2B. A magnified view focusing on the kinase domain complex by CaMKIIβ subunits is shown.

b, The inside of the spine is depicted before (left) and after (right) Ca^{2+} stimulation.

Uncropped blots

Supplementary Figure 3a

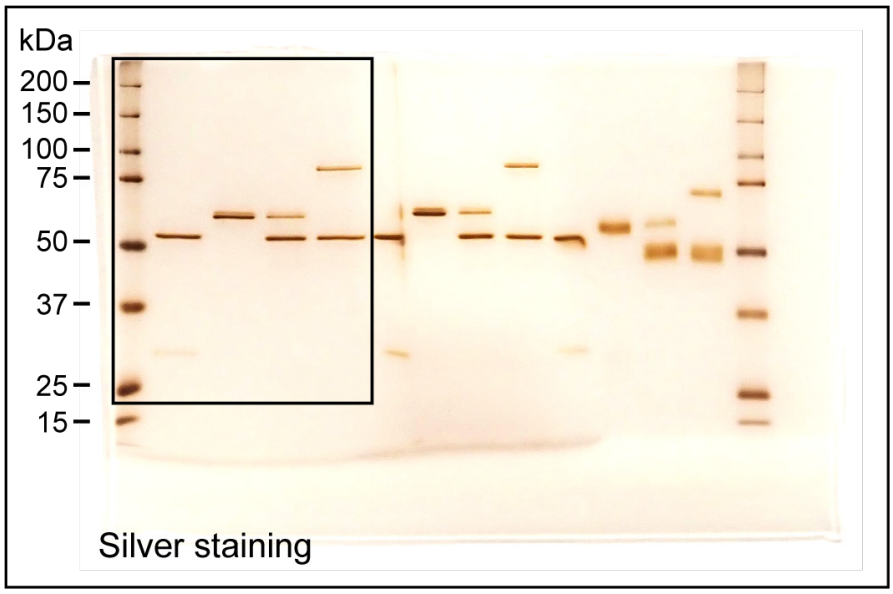

Supplementary Figure 3b

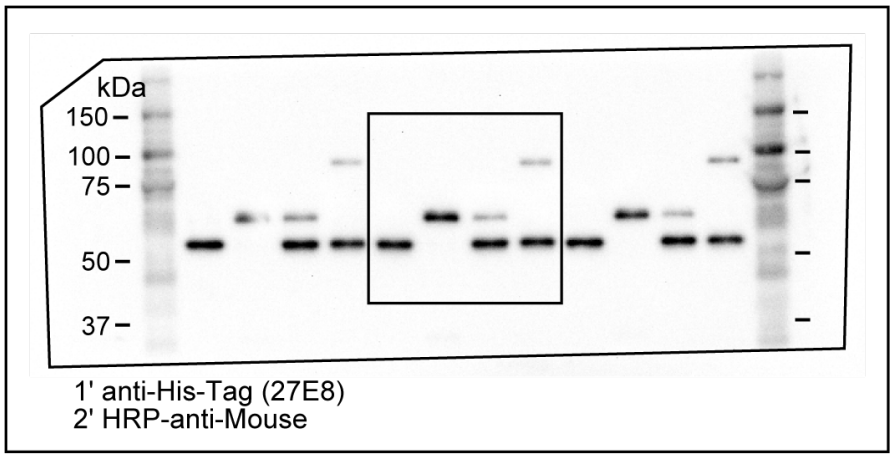

Supplementary Figure 8